Journal of Materials Chemistry A

Accepted Manuscript

ROYAL SOCIETY OF CHEMISTRY

www.rsc.org/materialsA

Graphical and textual abstract for the Table of contents entry

Sol-gel prepared copper chromium delafossite electrodes behave as stable and efficient photocathodes for water reduction without the need of co-catalysts.

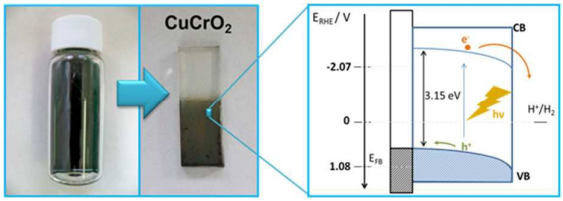

Journal of Materials Science A

COMMUNICATION

Sol-gel copper chromium delafossite thin films as stable oxide photocathodes for water splitting

Received 00th January 20xx,
Accepted 00th January 20xx

DOI: 10.1039/x0xx00000x

www.rsc.org/

Ana Korina Díaz-García[a], Teresa Lana-Villarreal[a] and Roberto Gómez[a,]*

Significant effort is being devoted to the study of photoactive electrode materials for artificial photosynthesis devices. In this context, photocathodes promoting water reduction based on earth-abundant elements and possessing stability under illumination should be developed. Here, the photoelectrochemical behavior of $CuCrO_2$ sol-gel thin film electrodes prepared on conducting glass is presented. The material, whose direct band gap is 3.15 eV, apparently presents a remarkable stability in both alkaline and acidic media. In 0.1 M $HClO_4$ the material is significantly photoactive, with IPCEs at 350 nm and 0.36 V vs. RHE of over 6% for proton reduction and 23% for oxygen reduction. This response was obtained in the absence of charge extracting layers or co-catalysts, suggesting substantial room for optimization. The photocurrent onset potential is equal to 1.06 V vs. RHE for both alkaline and acidic media, which guarantees its combination with different photoanodes such as Fe_2O_3 or WO_3, potentially yielding bias-free water splitting devices.

One of the current challenges faced by mankind is to find ways to harvest solar light and convert it into chemical energy due to the dainty situation of fossil fuels on earth. Water splitting seems to be one of the most convenient ways to reach this goal.[1-3] Hydrogen could play a very important role due to its potential use in clean energy applications.[4] As a consequence, achieving high efficiency in solar water photosplitting would contribute to convert our fossil fuel dependent society into another one whose development would be based on renewable energy.

Since the mid-1970s and initiated by the Fujishima and Honda's seminal work,[5] photoelectrochemistry has experienced a rapid development in the field of conversion of solar energy into chemical energy. If we refer only to the work done with oxide electrodes, the first 30-40 years of photoelectrochemistry development have focused on the study of some binary oxides together with a few ternary oxides (notably $SrTiO_3$).[6] Most of these electrode materials exhibited an n-type behavior with the development of anodic photocurrents in many cases associated with water photooxidation. In spite of the substantial effort done during all these years, no ideal photoanode has been found for water splitting, particularly if we think of devices in which the photoanode is combined with a dark cathode.

On the other hand, from a theoretical point of view, the development of tandem devices is preferable, as the maximum attainable efficiency is higher than in devices based on one photoelectrode.[7] This requires the development of stable photocathodes based on abundant materials. In this context, only a few binary oxides have been described to exhibit p-type behavior (mainly cobalt, nickel, and, particularly copper oxides).[8] It should be mentioned that the photoactivity of cobalt and nickel oxides in aqueous media is very weak. Copper oxides exist in two different oxidation states, Cu_2O and CuO. These two compounds have band gap energies of 2.0-2.2 eV and 1.3-1.6 eV, respectively. In addition, both oxides have high absorption coefficients over a significant portion of the solar spectrum and are environmentally friendly. In fact, there are some reports on the use of both Cu_2O and CuO for the photogeneration of hydrogen from water.[9,10] Nevertheless, copper oxides exhibit a rather poor chemical stability under illumination, as the large photocurrents that they develop are mostly associated to the reduction of copper oxides to metallic copper rather than to the reduction of water.

In principle, oxides with a more complex structure and composition (ternary and quaternary oxides) constitute an attractive alternative for the development of photoelectrodes (particularly photocathodes) potentially stable in aqueous environments. Among them, spinels (AB_2O_4), delafossites (ABO_2) and perovskites or ilmenites (ABO_3) are awakening an increasing interest in the last years in heterogeneous photocatalysis, as transparent conducting oxides, or as electrodes for both batteries and dye-sensitized solar cells.[11-18] Photoelectrochemical measurements with p-type semiconductor spinels have been performed mainly with $CaFe_2O_4$.[19-21] This material has shown significant stability and the ability to photogenerate hydrogen at relatively high potentials in alkaline aqueous solutions. Among

[a] Institut Universitari d'Electroquímica i Departament de Química Física, Universitat d'Alacant, Apartat 99, E-03080 Alicante, Spain. E-mail: Roberto.Gomez@ua.es

Electronic Supplementary Information (ESI) available: Experimental details, UV-vis absorbance spectrum for an FTO/CuCrO2 electrode, additional SEM image, linear scan voltammograms under transient 1 sun illumination and pho-tocurrent transients under 1 sun illumination in 0.1 M $HClO_4$, linear scan voltammograms under transient illumination in 0.1 M NaOH, long-term chronoamperometric experiments under transient illumination in 0.1 M $HClO_4$ and 0.1 M NaOH See DOI: 10.1039/x0xx00000x.

delafossites, photoelectrochemical studies have focused on $CuFeO_2$ and $CuRhO_2$,[22-25] while some reports have also appeared on perovskites such as $CuNbO_3$ and $LaFeO_3$.[26-28]

The delafossite $CuCrO_2$ has been reported to have a conduction band edge negative to the hydrogen evolution potential.[13] The photoelectrochemical behavior of $CuCrO_2$ has been examined on a few occasions with electrodes prepared in the form of pellets,[29] as single crystals[30] and from nanoparticles deposited on a conducting substrate.[31] In none of these works, the response of the electrodes under illumination was studied in detail and the preliminary results were characterized by the presence of large dark currents. The chemical stability of this oxide in contact with solutions of different pHs has also been highlighted.[15] In this work, we report on the behavior of $CuCrO_2$ thin film electrodes prepared by a sol-gel procedure with a focus on its structural, morphological and photoelectrochemical properties. Important features of this electrode material such as a high photocurrent onset potential, significant photoactivity and chemical stability are highlighted.

$CuCrO_2$ thin films were prepared on commercial fluorine-doped tin oxide (FTO) glass substrates by a sol-gel method[32] using $Cu(CH_3COO)_2{\cdot}H_2O$ and $Cr(NO_3)_3{\cdot}9H_2O$ as metallic precursors. The precursor solution was spin-coated on FTO and then the samples were annealed at 400 ^oC in air for 1 h. This procedure was repeated four times. Finally, the samples were post-annealed at 650 ^oC in N_2. The as prepared films were transparent and homogeneous (average thickness of 0.2 µm) and showed good adhesion. They presented a gray-green coloration. The UV-vis spectrum is characterized by a broad contribution through the entire visible region with two absorption bands at around 400 and 600 nm (Fig. S1, see ESI†). Qualitatively similar spectra have been reported for $CuCrO_2$ powders prepared by a high-temperature solid-state reaction.[31] These bands have been assigned to d-d transitions of octahedral Cr^{3+}. Therefore, they do not lead to charge separation and should not be linked to photoelectrochemical processes. More information on the electronic transitions relevant in photoelectrochemistry is provided by means of incident photon-to-current efficiency (IPCE) measurements (see below).

Fig. 1a shows the XRD patterns for an FTO conductive glass piece prior and after the deposition of a $CuCrO_2$ thin film. Apart from FTO, $CuCrO_2$ was the only phase detected in the thin film. As shown in Fig. 1b, the SEM image of the sample shows that it is composed of irregular polyhedral grains with an average diameter of 150 nm (see histogram as an inset). The particle arrangement is compact, which can be attributed to a densification due to the annealing treatment (Fig. S2, see ESI†).

One of the most notable features of this material is that it allows us to work in both strongly acidic and strongly alkaline solutions. First of all, the electrochemical characterization was done in the dark. As observed in Fig. 2a, over a wide potential range, the electrochemical response is characterized by the existence of small capacitive currents, which tend to be higher as the solution pH increases. Above 1.0 V a capacitive contribution similar to an accumulation region appears. In particular, in the alkaline medium the voltammogram presents a couple of peaks at around 0.8 V, together with a more developed accumulation region. Qualitatively similar voltammetric features have been described for a polycrystalline pellet electrode and they have been attributed to electrochemical oxygen intercalation/deintercalation (accompanied by oxidation/reduction of Cu^+/Cu^{2+}).[29] From a physical point of view, these currents could be interpreted as corresponding to the filling/emptying of either valence band (VB) states or surface states close to the VB edge. In this respect, it is worth noting that DFT calculations of the band structure of this and other delafossites indicate that the upper part of the VB mostly consists of Cu 3d states.[33]

Fig. 2b shows linear scan voltammograms performed under chopped illumination in 0.1 M $HClO_4$ saturated with either nitrogen or oxygen under otherwise identical conditions. They are characterized by the existence of very small dark currents (in agreement with the cyclic voltammograms shown in Fig. 2a)

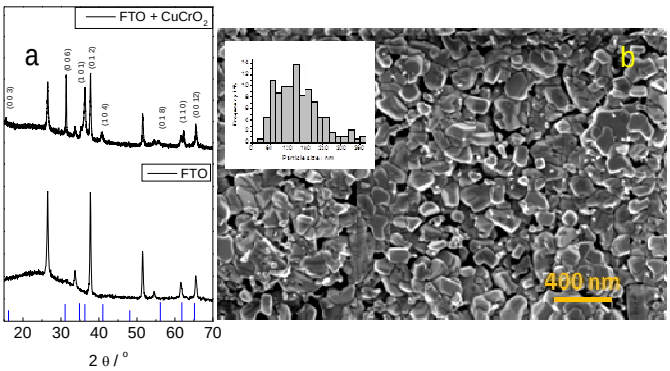

Fig. 1 (a) X-ray diffractograms for both the supported delafossite thin film and the FTO substrate. (b) SEM image for the $CuCrO_2$ thin film showing the grains and their size distribution (inset).

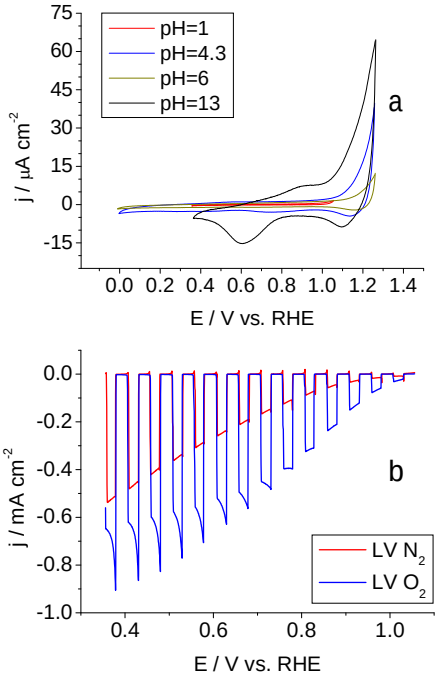

Fig. 2 (a) Cyclic voltammograms for a $CuCrO_2$ electrode in the dark at different pHs. Scan rate: 20 $mV{\cdot}s^{-1}$. (b) Linear scan voltammetry for a $CuCrO_2$ electrode in 0.1 M $HClO_4$ purged with either N_2 or O_2 under illumination with an ozone-free Xe arc lamp (0.65 $W{\cdot}cm^{-2}$). Scan rate: 5 $mV{\cdot}s^{-1}$.

together with cathodic photocurrents whose magnitude increases as the potential is made more negative. Both in the absence and in the presence of oxygen, the onset potential is located at around 1.06 V vs. RHE, which is among the highest values reported for photocathodes together with those of $LaFeO_3$[27] or $CuFeO_2$, although in the latter case, significant photocurrents were observed only in the presence of oxygen.[25] The response of the electrode under interrupted illumination was remarkably stable. No significant changes were observed in two subsequent linear scan voltammograms recorded under chopped illumination (see below).

Interestingly, the shape of the transients in the absence of oxygen does not show clear signs of electron trapping at the electrode surface, except in the more positive potential region in which the appearance of cathodic spikes upon illumination together with anodic spikes upon light interruption indicate otherwise. In the presence of oxygen, the photocurrent increases significantly and the spikes disappear, which attests an easier transfer of photogenerated electrons to oxygen than to water/protons. In addition, it is remarkable that the cathodic currents within each transient (associated to the reduction of oxygen) show a declining tendency for negative enough potentials, which should be associated to the limited solubility of oxygen and to the easy attainment of transport limitations. These measurements were repeated under one sun illumination (Figs. S3 and S4, see ESI†), leading to qualitatively similar results. It is remarkable though that in this case, the photocurrent was not observed to decrease over time in the presence of oxygen, in agreement with the lower rate of oxygen reduction prevailing in this case. In addition, the shape of the photocurrent transients for N_2-purged solutions shows clearly for 1 sun illumination the existence of cathodic spikes upon illumination together with anodic spikes upon light interruption. This indicates that electron trapping at the surface is one of the factors limiting the performance of this electrode material. Interestingly, the electron trapping sites would become saturated under sufficiently intense illumination and negative enough potentials as deduced from Fig. 2b (rectangular transients).

A behavior similar to that shown in Fig. 2b has been observed in both neutral and alkaline solutions (Fig. S5 for the $CuCrO_2$ response in 0.1 M NaOH, see ESI†). However, under the same illumination conditions, the photocurrent for water reduction was significantly higher in acidic solution, suggesting that a low pH may improve electron transfer toward aqueous species and/or facilitate electron transport toward the surface oxide. The latter could be linked to the fact that the oxide surface should be positively charged in contact with an acidic solution. It is important to signify that in photocatalytic experiments employing a sacrificial agent such as ethanol or glycerol, $CuCrO_2$ powders have been shown to be capable of generating hydrogen, being this process enhanced by the formation of heterojunctions with materials such as ZnO or WO_3 or by adding co-catalysts such as Pt or Au.[34]

In order to examine more thoroughly the stability of the $CuCrO_2$ electrodes, additional experiments were performed in both alkaline and acidic media. These experiments consisted in illuminating the electrodes at a constant applied potential while recording the photocurrent. The electrodes were submitted to three illuminations periods of 2.5 hours separated by half-hour dark periods (Fig. S6, see ESI†). As observed, in acidic media there is initially a photocurrent decay during the first hour of illumination, but a rather stable photocurrent is observed afterward. The stability of the electrode is better in 0.1 M NaOH. In this case the photocurrent transients only show a small decay during the first two 2.5-h illumination transients.

The p-type behavior of the as prepared electrodes was confirmed by performing Mott-Schottky plots (Fig. 3) at two different frequencies in the dark and under illumination. In fact, the $1/C^2$ vs. E plot shows the expected linear tendency and frequency dispersion. From the intercept with the abscissa axis, a value of 1.08 V_{RHE} is obtained for the flat band potential. It is worth noting that this value is close to that of the photocurrent onset, indicating that recombination is limited. In the same way, it is relevant that the flatband potential does not significantly shift upon illumination, which means that the density of trapped electrons under photostationary conditions when the illumination is intense does not induce a downward shift of the flatband potential.

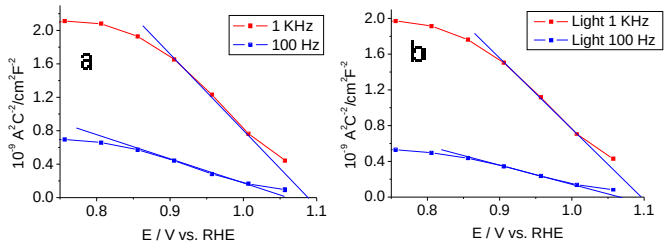

Fig. 3 Mott-Schottky plots (at two different frequencies) for a $CuCrO_2$ electrode in contact with an N_2-purged 0.1 M $HClO_4$ solution both in the dark (a) and under illumination (b) with an ozone-free Xe-arc lamp (0.65 W·cm^{-2}).

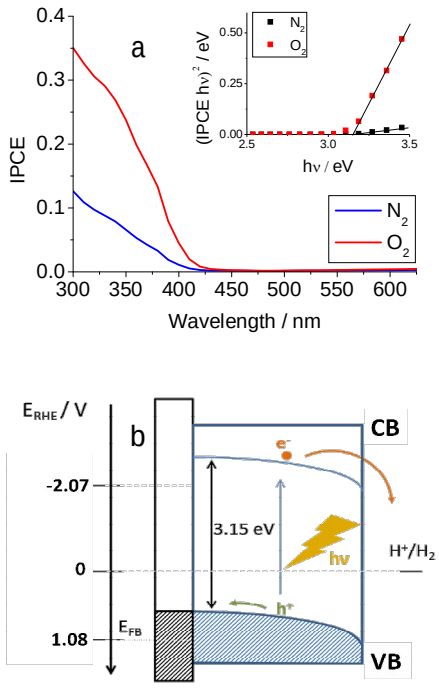

Fig. 4 (a) IPCE values as a function of the wavelength of the incident light for a $CuCrO_2$ electrode in 0.1 M $HClO_4$ purged with either N_2 or O_2. The inset shows the $(IPCE \cdot h\nu)^2$ vs. $h\nu$ plot. (b) Schematic band diagram for a $CuCrO_2$ electrode.

IPCE spectra were measured for both nitrogen-purged and oxygen-purged 0.1 M $HClO_4$ solutions at 0.36 V vs. RHE as shown in Fig. 4. In agreement with the observations under polychromatic illumination, the IPCE values are much higher in the presence of oxygen. Concretely, an IPCE of 6 % for proton reduction is measured at 350 nm while this value increases up to 23 % for oxygen reduction. Importantly, no photocurrents are generated for wavelengths over 430 nm, even when there is an absorption band at around 600 nm. This indicates that, in fact, the electronic excitation linked to this absorption band does not lead to spatial charge separation as indicated above.

Importantly, the IPCE values at wavelengths smaller than 430 nm allow us to determine the type of optical transition and the corresponding band gap. The inset in fig. 4a shows that a plot of $(IPCE \cdot h\nu)^2$ vs. $h\nu$ follows a linear tendency. By assuming that the IPCE is directly proportional to the absorption coefficient, $CuCrO_2$ is shown to be a direct semiconductor with a band gap of 3.15 eV, a value that is within the range of values reported in the literature for this material (between 2.95 and 3.18 eV). With the value of the bandgap and the flat band potential, a simple band diagram for the material can be drawn as shown in fig. 4b. The strong reducing character of the photogenerated electrons is apparent, suggesting the use of this material for the reduction of, not only water, but also CO_2.

It is important to signify that according to DFT calculations for copper delafossites, the upper part of the VB results from Cu 3d orbitals while the bottom of the conduction band (CB) is constituted by Cr 3d orbitals.[31,33] Therefore, photoexcitation should be considered chemically as the generation of Cu(II) species in the Cu subnetwork and Cr(II) species in the Cr subnetwork. The fact that the contribution of the Cu 3d orbitals to the CB bottom is minor may explain the stabilization of the Cu(I) oxidation state in the $CuCrO_2$ structure in contrast with the case of Cu_2O.

Conclusions

In summary, we have shown that sol-gel synthesized $CuCrO_2$ thin film electrodes behave as efficient photocathodes for water reduction. This material presents remarkable photoelectrochemical and chemical stability. The electrodes could be employed throughout the entire pH range and no photocurrent decay was observed in the course of the experiments. Importantly, the electrodes show significant photoactivity, even in the absence of co-catalysts. Another advantage of this material is its very high photocurrent onset potential (close to 1.06 V_{RHE}). Both its stability in different media and its high onset potential facilitate its potential use in tandem devices. It could indeed be combined with photoanodes resistant to either acidic (WO_3) or alkaline solutions (Fe_2O_3). Admittedly, $CuCrO_2$ has a too large bandgap as to harvest a significant part of the solar spectrum. In addition, the IPCE values need to be increased, particularly in the absence of oxygen. However, there are several ways that one could pursue in order to increase photoactivity. For instance, doping with other metals as to constitute mixed delafossites is an option. For example, the incorporation of Fe could be beneficial taking into account that $CuFeO_2$, with a band gap of 1.5-1.6 eV, has been reported to produce hydrogen (with Pt as a cocatalyst and using under- and overlayers).[22,25] Other options to decrease recombination would include the modification of the surface to avoid carrier trapping as well as doping with Mg^{2+} to improve carrier mobility. Finally, the use of underlayers and overlayers could also be explored as this strategy has been proven fruitful in the case of Cu_2O, $CuFeO_2$, and Fe_2O_3.[35]

Acknowledgements

We are grateful to the Spanish Ministry of Education and Competitiveness for financial support through project MAT2012-37676 (co-financed with FEDER funds by the European Union). A.-K.D.G. thanks the Mexican government (CONACYT) for the award of a doctoral grant.

Notes and references

1 J. Chen, D. Yang, D. Song, J. Jiang, A. Ma, M. Z. Hu and C. Ni, *J. Power Sources*, 2013**, 117**, 17879.
2 J.R. McKone, N.S. Lewis and H.B. Gray, *Chem. Mater.,* 2014, **26**, 407.
3 D. Kim, K.K. Sakimoto, D. Hong and P. Yang, *Angew. Chem. Int. Ed.* 2015, **54**, 3259.
4 P.P. Edwards, V.L. Kuznetsov and W.I.F. David, *Phil. Trans. R. Soc. A,* 2007, **365**, 1043.
5 A. Fujishima and K. Honda, *Nature,* 1972, **238**, 37.
6 K.J. Honda, *J. Photochem. Photobiol. A*, 2004, **166**, 63.
7 M.S. Prévot and K. Sivula, *J. Phys. Chem. C*, 2013, **117**, 17879.
8 C. Hu, K. Chu, Y. Zhao and W.Y. Teoh, *ACS Appl. Mater. Interfaces*, 2014, **6**, 18558.
9 A. Paracchino, V. Laporte, K. Sivula, M. Grätzel and E. Thimsen, *Nature Mater*., 2011**, 10**, 456.
10 C.-Y. Chiang; M.-H. Chang, H.S. Liu, C.Y. Tai, S. Ehrman, *Ind. Eng. Chem. Res.*, 2012, **51**, 5207.
11 D. Liu, W. Zhu, J. Trottier, C. Gagnon, F. Barray, A. Guerfi, A. Mauger, H. Groult, C.M. Julien, J.D. Goodenough and K. Zaghib, *RSC Adv.*, 2014, **4**, 154.
12 S. Wang, Z. Ding, X. Wang, *Chem. Commun.*, 2015, **51**, 1517.
13 P. Zhang, Y. Shi, M. Chi, J.N. Park, G.D. Stucky, E.W. McFarland and L. Gao, *Nanotechnology,* 2013*,* **24***,* 345704.
14 M. Yu, G. Natu, Z. Ji and J. Wu, *J. Phys. Chem. Lett.*, 2012, **3**, 1074.
15 A.M. Amrute, Z. Łodziana*,* C. Mondelli, F. Krumeich and J. Pérez-Ramírez, *J. Chem. Mater.*, 2013, **25**, 4423.
16 K. Toyoda, R. Hinogami, N. Miyata, M. Aizawa, *J. Phys. Chem. C*, 2015, **119**, 6495.
17 Y. Zhu, Y. Dai, K. Lai, Z. Li and B. Huang, *J. Phys. Chem. C*, 2013, **117**, 5593.
18 S. Royer, D. Duprez, F. Can, X. Courtois, C. Batiot-Dupeyrat, S. Laassiri and H. Alamdari, *Chem. Rev.*, 2014, **114**, 10292.
19 Y. Matsumoto, M. Omae, K. Sugiyama and E. Sato, *J. Phys. Chem*., 1987, **91**, 577.
20 S. Ida, K. Yamada, T. Matsunaga, H. Hagiwara, Y. Matsumoto and T. Ishihara, *J. Am. Chem. Soc.*, 2010, **132**, 17343.
21 K. Sekizawa, T. Nonaka, T. Arai and T. Morikawa, T. *ACS Appl. Mater. Interfaces*, 2014, **6**, 10969.
22 C.G. Read, Y. Park and K.-S. Choi, *J. Phys. Chem. Lett.*, 2012, **3**, 1872.
23 J. Gu, A. Wuttig, J.W. Krizan, Y. Hu, Z.M. Detweiler, R.J. Cava and A.B. Bocarsly, *J. Phys. Chem. C*, 2013, **117**, 12415.
24 J. Gu, Y. Yan, J.W. Krizan, Q.D. Gibson, Z.M. Detweiler, R.J. Cava and A.B. Bocarsly, *J. Am. Chem. Soc.*, 2014, **136**, 830.
25 M.S. Prévot, N. Guijarro, K. Sivula, *ChemSusChem,* 2015, **8**, 1359.

26 U.A. Joshi, A.M. Palasyuk and P.A. Maggard, *J. Phys. Chem. C*, 2011, **115**, 13534.
27 V. Celorrio, K. Bradley, O.J. Weber, S.R. Hall and D.J. Fermín, *ChemElectroChem*, 2014, **1**, 1667.
28 K.J. May, D.P. Fenning, T. Ming and W.T. Hong, D. Lee, K.A. Stoerzinger, M.D. Biegalski, A.M. Kolpak and Y. Shao-Horn, *J. Phys. Chem. Lett*., 2015, **6**, 977.
29 W. Ketir, A. Bouguelia and M. Trari, *Desalination*, 2009, **244**, 144.
30 W. Ketir, S. Saadi and M. Trari, *J. Solid State Electrochem.,* 2012, **16**, 213.
31 Y. Ma, X. Zhou, Q. Ma, A. Litke, P. Liu, Y. Zhang, C. Li and E.J.M. Hensen, *Catal. Lett.,* 2014, **144**, 1487.
32 H.-Y. Chen and K.-P. Chang, *ECS J. Solid State Sci. Technol.,* 2013, **2**, 76.
33 M.-S. Miao, S. Yarbro, P.T. Barton and R. Seshadri, *Phys. Rev. B*, 2014, **89**, 045306.
34 S. Saadi, A. Bouguelia and M. Trari, *Solar Energy*, 2006, **80**, 272.
35 L. Steier, I. Herraiz-Cardona, S. Gimenez, F. Fabregat-Santiago, J. Bisquert, S.D. Tilley and M. Grätzel, *Adv. Funct. Mater.,* 2014, **24**, 7681.